

## Surface relaxation of topological insulators: Influence on the electronic structure

N. Fukui,<sup>1</sup> T. Hirahara,<sup>1,\*</sup> T. Shirasawa,<sup>2</sup> T. Takahashi,<sup>2</sup> K. Kobayashi,<sup>3</sup> and S. Hasegawa<sup>1</sup>

<sup>1</sup>*Department of Physics, University of Tokyo, 7-3-1 Hongo, Bunkyo-ku, Tokyo 113-0033, Japan*

<sup>2</sup>*Institute for Solid State Physics, University of Tokyo, 5-1-5 Kashiwanoha, Kashiwa 277-8581, Japan*

<sup>3</sup>*Department of Physics, Ochanomizu University, 2-1-1 Otsuka, Bunkyo-ku, Tokyo 112-8610, Japan*

(Received 24 January 2012; published 20 March 2012)

The surface structure of topological insulators  $\text{Bi}_2\text{Te}_3(111)$  and a single bilayer bismuth on it was studied by low-energy electron-diffraction analysis. The topmost quintuple layer of  $\text{Bi}_2\text{Te}_3$  showed only a slight relaxation ( $\sim 1\%$  contraction). On the other hand, the bilayer Bi was strongly distorted compared to bulk Bi (3.5% in-plane contraction and  $\sim 7\%$  out-of-plane expansion). First-principles calculation reveals that this distortion has a large influence on the electronic structure and can enlarge the band gap.

DOI: [10.1103/PhysRevB.85.115426](https://doi.org/10.1103/PhysRevB.85.115426)

PACS number(s): 68.35.-p, 73.20.-r

Topological insulators (TIs) have been attracting many researchers since their existence was predicted theoretically<sup>1-3</sup> and later confirmed experimentally in a  $\text{HgTe}/\text{CdTe}$  quantum well as a two-dimensional TI,<sup>4</sup> and  $\text{BiSb}$  alloy as a three-dimensional TI.<sup>5</sup> One of the most remarkable and interesting features of TIs is that the bulk is an insulator with a band gap, while there are spin-split gapless bands localized at the edge or surface. Furthermore, these edge states form a Dirac cone in the simplest case, which indicates the high carrier mobility due to the zero effective mass. Therefore they are interesting not only in terms of basic science but also in industrial applications.

Bismuth telluride ( $\text{Bi}_2\text{Te}_3$ ) is currently one of the most extensively studied three-dimensional TIs along with  $\text{Bi}_2\text{Se}_3$ .<sup>6-8</sup> The Te trigonal-lattice layer and Bi trigonal-lattice layer alternate to form a quintuple layer (QL) [see Figs. 1(b) and 1(c)], which is the stacking unit along the (111) direction. The interaction between neighboring QLs is weak (the gap between QLs is called the van der Waals gap) and therefore they can easily be cleaved along the (111) plane. It has been known that surface relaxation has a significant influence on the electronic structure of these layered materials. For example, it was debated whether the surface of  $\text{Bi}(111)$ , which is another stacking material, has a significant surface relaxation or not in relation with the spin-orbit split-band dispersion. In Ref. 9, it was shown that the topmost Bi bilayer was nearly isolated from the underlying bulk, but the low-energy electron-diffraction (LEED) analysis shown in Ref. 10 indicated that there was only slight relaxation. In a more recent study, it was found that by depositing Ag on  $\text{Bi}_2\text{Se}_3$ , intercalation takes place and Ag goes inside the crystal and resides between the first and second QLs.<sup>11</sup> They predicted the expansion of the van der Waals gaps and the detachment of topmost QLs from the bulk crystal. It was concluded that this will lead to a relocation of the topological state beneath the detached quintuple layers. So it seems that understanding the surface relaxation is crucial to discuss the surface-state band dispersion accurately.

A single bilayer  $\text{Bi}(111)$  was previously theoretically predicted as a candidate of a two-dimensional TI.<sup>12</sup> The bilayer (BL) of Bi consists of two atomic layers and forms a hexagonal lattice. It cannot be formed on a  $\text{Si}(111)$  surface due to the formation of a pseudocubic {012}-oriented film below the critical coverage of  $\sim 6$  BL.<sup>13</sup> But recent research confirmed that  $\text{Bi}(111)$  can be grown on  $\text{Bi}_2\text{Te}_3(111)$  from 1 BL (Ref. 14)

due to the relatively small lattice mismatch and similar crystal structure. Although it was shown that this Bi 1 BL/ $\text{Bi}_2\text{Te}_3$  (Bi1BL hereafter) has a quite intriguing band dispersion, it is not still clear how the atomic structure is altered from the bulk  $\text{Bi}(111)$  due to this lattice mismatch.

As mentioned above, there are many works that have investigated the electronic structure of TIs and explored the exotic band dispersion. On the other hand, although it seems important to identify the atomic structures of TIs precisely, there are hardly any reports on them. Therefore in this paper, we studied the surface structures of  $\text{Bi}_2\text{Te}_3(111)$  and Bi1BL by LEED analysis (symmetrized automated tensor LEED, SATLEED). We found that the topmost quintuple layer of  $\text{Bi}_2\text{Te}_3(111)$  showed only a small relaxation compared to the bulk. In contrast, Bi1BL showed drastic expansion along the surface-normal direction which is likely a result of the contraction in the in-plane lattice constants. *Ab initio* calculations were also performed and the result indeed suggests that the band dispersion will change according to the degree of the surface relaxation of the Bi1BL.

All the film fabrication and measurements were done *in situ*. First, a clean  $\text{Si}(111)-7 \times 7$  surface was prepared on an *n*-type substrate (P-doped, 1–10  $\Omega$  cm at room temperature) by a cycle of resistive heat treatments. Then in a Te-rich atmosphere, Bi was deposited on the substrate at 215 °C to grow an 18 QL  $\text{Bi}_2\text{Te}_3$  thin film. After postannealing for 100 min at the same temperature, the  $\text{Bi}_2\text{Te}_3(111)$  sample was obtained. The Bi1BL sample was prepared by depositing additional Bi on the  $\text{Bi}_2\text{Te}_3(111)$  film at room temperature. The surface structure analysis of  $\text{Bi}_2\text{Te}_3$  and Bi1BL was performed with the LEED intensity vs voltage (*IV*) analysis. *IV* curves were obtained at 80 K, and their variations were within 1 K during the measurements. The LEED patterns with incident energy from 80 to 400 eV were recorded in steps of 1 eV by a digital CCD camera. *IV* curves of 14 inequivalent diffraction spots were obtained. In order to determine the surface structure, we calculated the *IV* curves in the tensor LEED to fit the experimental *IV* curves using the SATLEED package of Barbieri/Van Hove.<sup>15</sup> As shown in Figs. 1(c) and 3(c), each atomic layer was treated differently according to their environments. The in-plane lattice constant was determined from positions of the LEED spots. Angular momentum up to 17 ( $l_{\text{max}} = 17$ ) was taken into account because of the strong

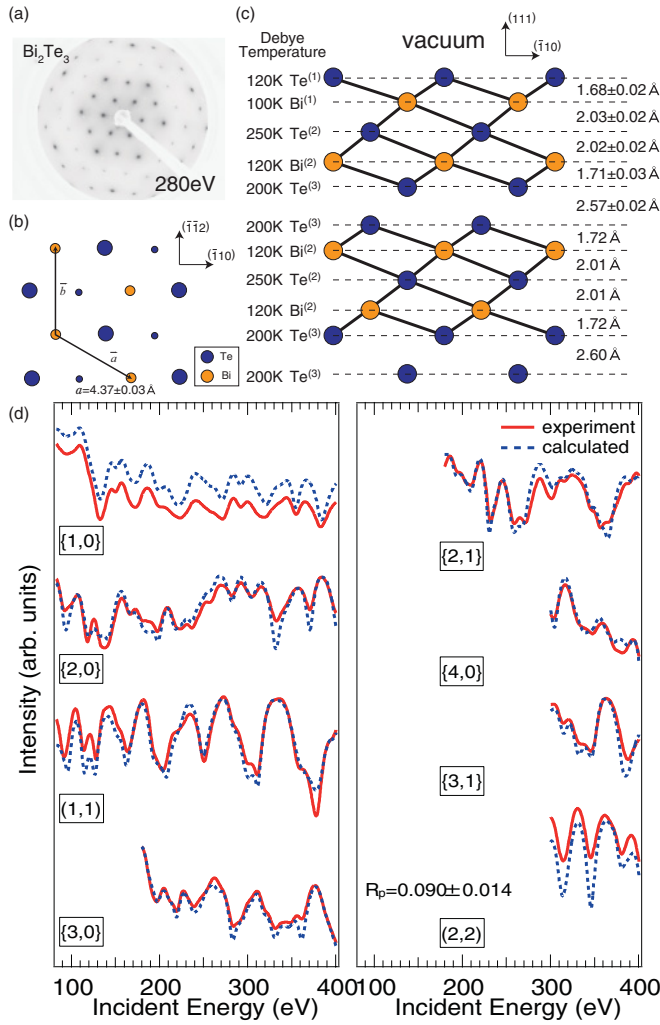


FIG. 1. (Color online) (a) LEED pattern of the  $1 \times 1$   $\text{Bi}_2\text{Te}_3(111)$  surface at 80 K. [(b), (c)] Top (b) and side (c) view of the  $\text{Bi}_2\text{Te}_3(111)$  surface. The orange (light gray) circles represent Bi and blue (dark gray) ones represent Te. (d)  $IV$  curves of the  $\text{Bi}_2\text{Te}_3(111)$  surface. The solid lines are experimentally obtained ones and dashed lines are calculated ones.

scattering of the heavy Bi atom ( $Z = 83$ ). Considering the mean penetration depth of the incident electrons of  $\sim 10 \text{ \AA}$ , only the surface QL (and the additional Bi 1BL in the case of the Bi1BL sample) was allowed to relax. In search of the optimal structure, the out-of-plane lattice constant of the underlying QLs was changed from 2% contraction to 2% expansion compared to the bulk value, and the Debye temperature of each atom was changed in steps of 10 K from 50 K up to 300 K.

First-principles calculations were performed using the WIEN2K computer code on the basis of the augmented plane wave + local orbitals method taking into account the spin-orbit interaction, and the generalized gradient approximation<sup>17</sup> has been used for the description of exchange-correlation potential.

Figure 1(a) is a LEED pattern of the  $1 \times 1$   $\text{Bi}_2\text{Te}_3(111)$  surface. Figure 1(d) shows the experimentally observed  $IV$  curves of symmetrically inequivalent spots and calculated ones for the optimized surface structure. Despite the  $p3m1$

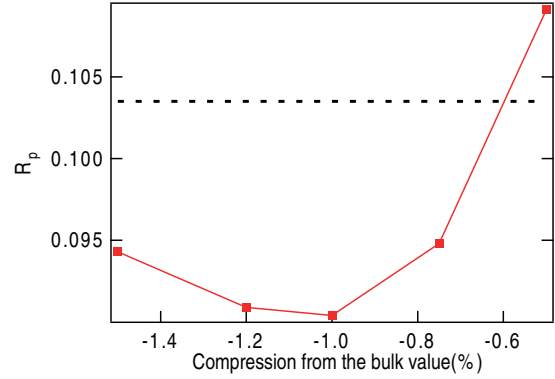


FIG. 2. (Color online)  $R$  factor vs the out-of-plane lattice compression of  $\text{Bi}_2\text{Te}_3$ . The dashed line indicates the upper limit of the reliability of  $R_p$ . The data points below this line is the uncertainty of the lattice constant.

symmetry of the  $\text{Bi}_2\text{Te}_3(111)$  surface, the symmetrically inequivalent spots, such as (1,0) and (0,1) spots, exhibited almost the same  $IV$  curves. This is because there are twin domains on the surface, which are related by a  $180^\circ$  rotation, and thus their superposition leads to the apparent twofold symmetry. Taking this double-domain surface into account, we took the average of the  $IV$  curves both in the calculation and in the experimental data such that  $\{h,k\}$  is the average of  $(h,k)$  and  $(k,h)$  spots. Note that spots having the same mirror indices of  $h$  and  $k$  do not need averaging.

As shown in Fig. 1(d), there was excellent agreement between the measured  $IV$  curves and calculated ones for the  $\text{Bi}_2\text{Te}_3$  surface. The Pendry reliability factor ( $R$  factor,  $R_p$ ), which determines the degree of the agreement between the experimental  $IV$  curves and the calculated ones,<sup>16</sup> was 0.090. The in-plane lattice constant was determined as  $4.37 \pm 0.03 \text{ \AA}$ , which is equal to the bulk value  $4.38 \text{ \AA}$  within the error [Fig. 1(b)]. Figure 2 shows the dependence of  $R_p$  on the out-of-plane lattice constant for the layers below the topmost QL. The optimized out-of-plane lattice constant was  $30.19 \pm 0.18 \text{ \AA}$ , which was slightly smaller than that of bulk  $\text{Bi}_2\text{Te}_3$ , which is  $30.49 \text{ \AA}$ , by  $1 \pm 0.3\%$ .<sup>18</sup>

The interlayer lattice parameters for the first QL are shown in Fig. 1(c) together with the Debye temperature. It can be seen that  $\text{Te}^{(1)}\text{-Bi}^{(1)}$  atomic plane distance shrinks a little bit and the distance of the van der Waals gap (between  $\text{Te}^{(3)}\text{-Te}^{(3)}$ ) becomes a bit smaller than the bulk value. The change is again only within 2%. Therefore it seems that there is only a slight relaxation at the topmost QL for  $\text{Bi}_2\text{Te}_3(111)$ . Concerning the Debye temperature also shown in Fig. 1(c), the atoms near the surface tend to have lower Debye temperatures than those inside the bulk crystal [the bulk Debye temperature of  $\text{Bi}_2\text{Te}_3$  (not layer resolved) is 160 K (Ref. 20)]. This tendency can be seen in many single-crystal surfaces, such as  $\text{NaCl}(100)$ ,  $\text{KCl}(100)$  (Ref. 19), and  $\text{Bi}(111)$ .<sup>10</sup> As a consequence, there seems to be no significant relaxation on the surface of  $\text{Bi}_2\text{Te}_3$ .

Now let us move on to the Bi1BL sample. The LEED pattern is shown in Fig. 3(a) and is very much similar to that of the pristine  $\text{Bi}_2\text{Te}_3(111)$  [Fig. 1(a)]. This implies that the deposited Bi(111) 1 BL preserves the in-plane lattice constant of  $\text{Bi}_2\text{Te}_3$ ,  $4.37 \pm 0.03 \text{ \AA}$  [Fig. 3(b)]. By comparing Figs. 1(d) and 3(d), it is found that the deposition of Bi1BL

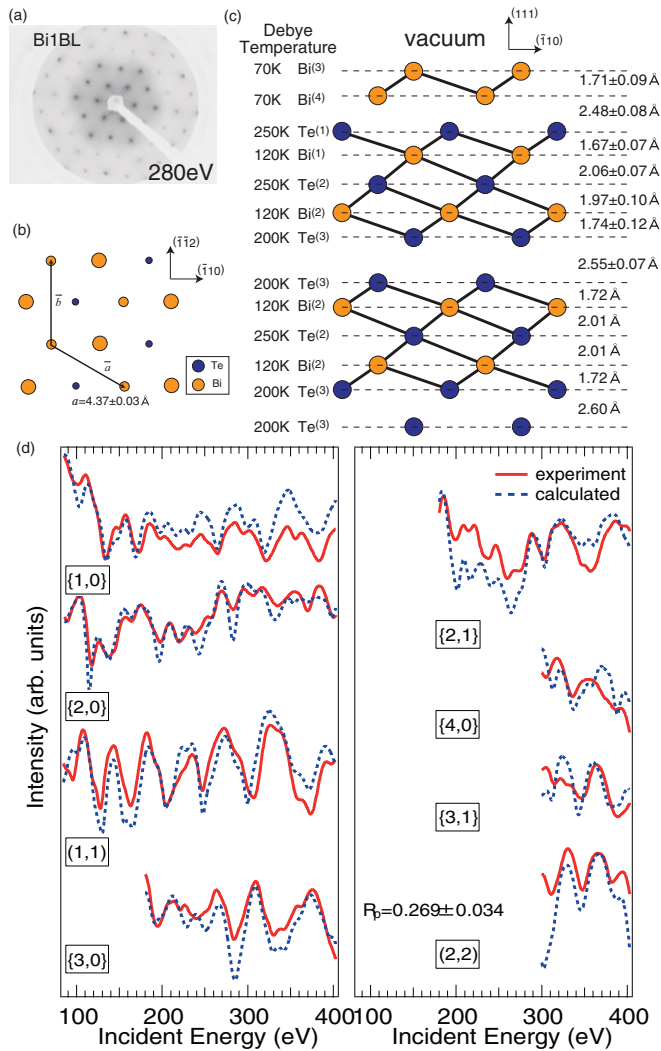


FIG. 3. (Color online) (a) LEED pattern of the bilayer Bi on Bi<sub>2</sub>Te<sub>3</sub>. [(b),(c)] Top (b) and side (c) view of the Bi bilayer on Bi<sub>2</sub>Te<sub>3</sub>. The orange (light gray) circles represent Bi and the blue (dark gray) ones represent Te. (d) *IV* curves of the bismuth bilayer on Bi<sub>2</sub>Te<sub>3</sub>. The solid lines are experimentally obtained ones and the dashed lines are calculated ones.

affected the shape of the *IV* curves a little bit. In particular, the {2,1} spot shows some change. The best-fit model is shown in Figs. 3(c) and 3(d) shows that the calculated *IV* curves agree fairly well with the experimental ones. The minimum  $R_p$  was 0.269 and the optimized out-of-plane lattice constant for the layers under the second QL was the same as that of the Bi<sub>2</sub>Te<sub>3</sub> sample. The optimized intrabilayer (Bi<sup>(3)</sup>-Bi<sup>(4)</sup>) and interbilayer (Bi<sup>(4)</sup>-Te<sup>(1)</sup>) distance in Bi1BL was 1.71 and 2.48 Å, respectively. The corresponding values for bulk Bi are 1.59 and 2.35 Å, meaning that the Bi1BL is expanded by 7.5 and 5.5%, respectively. Figure 4 shows the  $R_p$  dependence on these parameters. There was no significant relaxation in the surface-normal direction in the underlying Bi<sub>2</sub>Te<sub>3</sub>. As a whole, the expansion is  $7 \pm 3\%$ . Compared to the Te<sup>(3)</sup>-Te<sup>(3)</sup> distance between QLs (2.55 Å), the topmost interlayer Bi<sup>(4)</sup>-Te<sup>(1)</sup> distance (2.48 Å) is smaller [Fig. 3(c)]. This can be qualitatively understood as follows. A calculation based on the density functional theory suggests that both

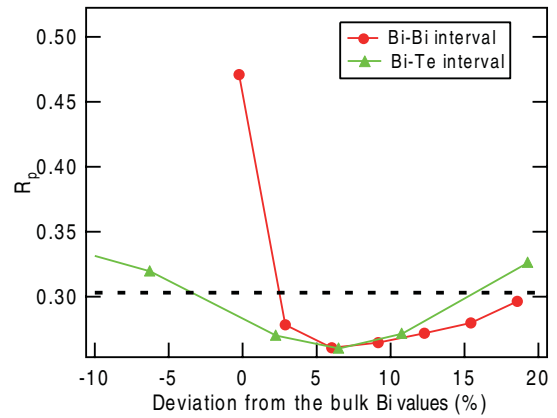


FIG. 4. (Color online)  $R$  factor as a function of the lattice expansion for the intrabilayer Bi distance (red or dark gray circles) and the distance between the bottom of the Bi bilayer and the topmost Te layer of Bi<sub>2</sub>Te<sub>3</sub> (green or light gray triangles). The values are compared to bulk Bi values. The dashed line indicates the upper limit of the trustworthy  $R_p$  value.

covalent bonds and ionic bonds are formed between Bi atoms and Te atoms in a Bi<sub>2</sub>Te<sub>3</sub> QL.<sup>21</sup> Since the electronegativity of Te is a little larger than Bi, Te atoms are negatively charged and Bi atoms are positively charged. Thus when the Te layer is replaced by a Bi layer, it can be expected that the Bi<sup>(4)</sup>-Te<sup>(1)</sup> distance will be shorter than the Te<sup>(3)</sup>-Te<sup>(3)</sup> (QL-QL) distance. Interestingly, Te<sup>(1)</sup> of the Bi<sub>2</sub>Te<sub>3</sub> surface shows the same Debye temperature as Te<sup>(2)</sup> in Fig. 3(c), which is in contrast to that in the pristine Bi<sub>2</sub>Te<sub>3</sub> [see Fig. 1(c)]. Probably this is because the Bi overlayer makes a similar environment for Te<sup>(1)</sup> and Te<sup>(2)</sup>; both are in between Bi layers. The Debye temperatures of Bi<sup>(3)</sup> and Bi<sup>(4)</sup> are both 70 K, which were lower than that of Bi<sup>(1)</sup>. It is notable that these values are consistent with the results of the preceding experiments on the single-crystal Bi (111) surface.<sup>10</sup>

The Bi 1BL on Bi<sub>2</sub>Te<sub>3</sub> is commensurate to the Bi<sub>2</sub>Te<sub>3</sub> surface, meaning that the parallel lattice constant of Bi<sub>2</sub>Te<sub>3</sub> is smaller than that of bulk Bi by 3.5%. As a result, Bi1BL is elongated to the surface normal by  $7 \pm 3\%$  so that the volume will be conserved. The calculated Poisson's ratio is  $0.5 \pm 0.1$ . This value exceeds the Poisson's ratio of bulk Bi (0.33) and is almost the maximum of the theoretically possible Poisson's ratio 0.5 for an elastic material. Therefore we can say that Bi1BL is strongly distorted. Such distortion (in-plane lattice contraction and out-of-plane lattice expansion) is also qualitatively consistent with the actual structure used to calculate the band dispersion shown in Ref. 14.<sup>22</sup>

In order to understand the influences of the Bi lattice distortion on the electronic structure, we performed first-principles calculations for the single bilayer Bi. Figures 5(a) and 5(b) show the band structures of a freestanding Bi bilayer along the high symmetry lines in the surface Brillouin zone [inset in Fig. 5(a)]. The distance between Bi layers is determined by minimizing the total energy, while the in-plane lattice constant is fixed. The optimized distances are close to the experimental values of 1.59 and 1.71 Å for the bulk Bi and the 1 BL Bi on the Bi<sub>2</sub>Te<sub>3</sub> substrate in this work, respectively. The band gap is 0.1 and 0.4 eV for the former

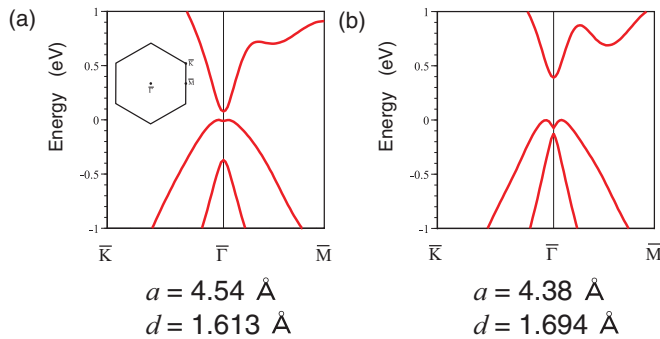


FIG. 5. (Color online) Calculated band structures of the single bilayer Bi with various lattice constants.  $a$  is the in-plane lattice constant and  $d$  is the distance between the two bismuth layers. The inset in (a) shows the Brillouin zone with high symmetry points.

(a) and latter (b) case, respectively. It can be easily recognized that the in-plane distortion has a great influence on the band structure. A wide energy gap of a TI film makes it easier to control the characteristics of the electrical conductivity of the edge states by electron or hole doping. Therefore, it seems like

a good idea to grow a bilayer Bi on a substrate with a smaller in-plane lattice constant such as  $\text{Bi}_2\text{Te}_3$  because the horizontal contraction and vertical expansion will be achieved in a natural way and thus result in the larger band gap, although the effects of the substrate itself also need to be taken into account.<sup>14</sup>

In summary, we have investigated the surface atomic structure of  $\text{Bi}_2\text{Te}_3$  and Bi1BL by LEED  $IV$  analysis. It revealed a slight contraction of the surface of  $\text{Bi}_2\text{Te}_3$  along the surface normal and the significant contraction (expansion) for the in-plane (out-of-plane) lattice parameters of bilayer Bi. Our *ab initio* calculations suggested that the strong distortion of the Bi bilayer helps obtain a wider energy gap, which is an advantage in easily tuning the properties of a topological insulator.

We thank Gustav Bihlmayer for discussions. This work has been supported by Grants-In-Aid from Japan Society for the Promotion of Science (22656011, 23686007) and JGC-S Scholarship Foundation. The LEED  $IV$  measurements were performed under the proposal number of ISSP domestic joint research A223 (2011).

\*hirahara@surface.phys.s.u-tokyo.ac.jp

<sup>1</sup>C. L. Kane and E. J. Mele, *Phys. Rev. Lett.* **95**, 226801 (2005).

<sup>2</sup>C. L. Kane and E. J. Mele, *Phys. Rev. Lett.* **95**, 146802 (2005).

<sup>3</sup>B. A. Bernevig and S.-C. Zhang, *Phys. Rev. Lett.* **96**, 106802 (2006).

<sup>4</sup>M. König, S. Wiedmann, C. Brüne, A. Roth, H. Buhmann, L. W. Molenkamp, X.-L. Qi, and S.-C. Zhang, *Science* **318**, 766 (2007).

<sup>5</sup>D. Hsieh, D. Qian, L. Wray, Y. Xia, Y. S. Hor, R. J. Cava, and M. Z. Hasan, *Nature (London)* **452**, 970 (2008).

<sup>6</sup>H. Zhang, C.-X. Liu, X.-L. Qi, X. Dai, Z. Fang, and S.-C. Zhang, *Nat. Phys.* **5**, 438 (2009).

<sup>7</sup>Y. Xia, D. Qian, D. Hsieh, L. Wray, A. Pal, H. Lin, A. Bansil, D. Grauer, Y. S. Hor, R. J. Cava, and M. Z. Hasan, *Nat. Phys.* **5**, 398 (2009).

<sup>8</sup>Y. L. Chen, J. G. Analytis, J.-H. Chu, Z. K. Liu, S.-K. Mo, X. L. Qi, H. J. Zhang, D. H. Lu, X. Dai, Z. Fang, S. C. Zhang, I. R. Fisher, Z. Hussain, and Z.-X. Shen, *Science* **325**, 178 (2009).

<sup>9</sup>C. R. Ast and H. Höchst, *Phys. Rev. B* **67**, 113102 (2003).

<sup>10</sup>H. Monig, J. Sun, Y. M. Koroteev, G. Bihlmayer, J. Wells, E. V. Chulkov, K. Pohl, and P. Hofmann, *Phys. Rev. B* **72**, 085410 (2005).

<sup>11</sup>M. Ye, S. V. Eremeev, K. Kuroda, M. Nakatake, S. Kim, Y. Yamada, E. E. Krasovskii, E. V. Chulkov, M. Arita, H. Miyahara, T. Maegawa, K. Okamoto, K. Miyamoto, T. Okuda,

K. Shimada, H. Namatame, M. Taniguchi, Y. Ueda, and A. Kimura, e-print [arXiv:1112.5869](https://arxiv.org/abs/1112.5869).

<sup>12</sup>S. Murakami, *Phys. Rev. Lett.* **97**, 236805 (2006).

<sup>13</sup>T. Nagao, J. T. Sadowski, M. Saito, S. Yaginuma, Y. Fujikawa, T. Kogure, T. Ohno, Y. Hasegawa, S. Hasegawa, and T. Sakurai, *Phys. Rev. Lett.* **93**, 105501 (2004).

<sup>14</sup>T. Hirahara, G. Bihlmayer, Y. Sakamoto, M. Yamada, H. Miyazaki, S.-i. Kimura, S. Blugel, and S. Hasegawa, *Phys. Rev. Lett.* **107**, 166801 (2011).

<sup>15</sup>M. A. Van Hove, W. Moritz, H. Over, P. J. Rous, A. Wander, A. Barbieri, N. Materer, and U. Starke, *Surf. Sci. Rep.* **19**, 191 (1993).

<sup>16</sup>J. B. Pendry, *J. Phys. C* **13**, 937 (1980).

<sup>17</sup>J. P. Perdew, A. Ruzsinszky, G. I. Csonka, O. A. Vydrov, G. E. Scuseria, L. A. Constantin, X. Zhou, and K. Burke, *Phys. Rev. Lett.* **100**, 136406 (2008).

<sup>18</sup>S. Nakajima, *J. Phys. Chem. Solids* **24**, 479 (1963).

<sup>19</sup>J. Vogt and H. Weiss, *Surf. Sci.* **491**, 155 (2001).

<sup>20</sup>G. E. Shoemaker, J. A. Rayne, and R. W. Ure Jr., *Phys. Rev.* **185**, 1046 (1969).

<sup>21</sup>S. K. Mishra, S. Satpathy, and O. Jepsen, *J. Phys.: Condens. Matter* **9**, 461 (1997).

<sup>22</sup>G. Bihlmayer (private communication).